PNAS Nexus, 2023, 2, 1–10
https://doi.org/10.1093/pnasnexus/pgad092
Advance access publication 22 March 2023
Research Report

Acylated plastoquinone is a novel neutral lipid accumulated in cyanobacteria

Toshiki Ishikawa[a], Shunya Takano[b], Riko Tanikawa[c], Takashi Fujihara[d], Kimie Atsuzawa[d], Yasuko Kaneko[e] and Yukako Hihara[b,*]

[a]Department of Environmental Science and Technology, Graduate School of Science and Engineering, Saitama University, Saitama 338-8570, Japan
[b]Department of Biochemistry and Molecular Biology, Graduate School of Science and Engineering, Saitama University, Saitama 338-8570, Japan
[c]Department of Biochemistry and Molecular Biology, Faculty of Science, Saitama University, Saitama 338-8570, Japan
[d]Comprehensive Analysis Center for Science, Saitama University, Saitama 338-8570, Japan
[e]Department of Natural Science, Faculty of Education, Graduate School of Science and Engineering, Saitama University, Saitama 338-8570, Japan
*To whom correspondence should be addressed: Email: hihara@mail.saitama-u.ac.jp
Edited By: Edward Bayer

Abstract

Although cyanobacteria do not possess bacterial triacylglycerol (TAG)-synthesizing enzymes, the accumulation of TAGs and/or lipid droplets has been repeatedly reported in a wide range of species. In most cases, the identification of TAG has been based on the detection of the spot showing the mobility similar to the TAG standard in thin-layer chromatography (TLC) of neutral lipids. In this study, we identified monoacyl plastoquinol (acyl PQH) as the predominant molecular species in the TAG-like spot from the unicellular *Synechocystis* sp. PCC 6803 (S.6803) as well as the filamentous *Nostocales* sp., *Nostoc punctiforme* PCC 73102, and *Anabaena* sp. PCC 7120. In S.6803, the accumulation level of acyl PQH but not TAG was affected by deletion or overexpression of *slr2103*, indicating that acyl PQH is the physiological product of Slr2103 having homology with the eukaryotic diacylglycerol acyltransferase-2 (DGAT2). Electron microscopy revealed that cyanobacterial strains used in this study do not accumulate lipid droplet structures such as those observed in oleaginous microorganisms. Instead, they accumulate polyhydroxybutyrate (PHB) granules and/or aggregates of alkane, free C16 and C18 saturated fatty acids, and low amounts of TAG in the cytoplasmic area, which can be detected by staining with a fluorescent dye specific to neutral lipids. Unlike these lipophilic materials, acyl PQH is exclusively localized in the membrane fraction. There must be DGAT2-like enzymatic activity esterifying de novo-synthesized C16 and C18 fatty acids to PQH_2 in the thylakoid membranes.

Keywords: acyl plastoquinone, cyanobacteria, diacylglycerol acyltransferase-2, neutral lipids, triacylglycerol

Significance Statement

For a long time, there has been a controversy over the accumulation of neutral lipids in cyanobacteria lacking bacterial triacylglycerol (TAG)-synthesizing enzymes. In this study, we identified a novel neutral lipid, monoacylated plastoquinol (acyl PQH), as the physiological product of the diacylglycerol acyltransferase-2 (DGAT2)-like protein Slr2103 and as the predominant component of the TAG-like spot detected by TLC of cyanobacterial neutral lipids. Our data resolved the long-standing question about the accumulation of neutral lipids in cyanobacteria. Acyl PQH is detected not only in *Synechocystis* but also in *Nostocales* species, and the DGAT2-like proteins are widely distributed among the phylum, indicating that the enzymatic production of the novel neutral lipid class has conserved functions in cyanobacteria.

Introduction

Cyanobacteria have been recognized as a promising platform for biofuel production, and various attempts of metabolic engineering have been made to increase the productivity of fatty acids and their derivatives (1). However, little is known about whether and how naturally occurring cyanobacteria accumulate triacylglycerols (TAGs), which is the common storage lipid in most organisms. Cyanobacteria do not possess wax ester synthase/acyl coenzyme A:diacylglycerol acyltransferase (WS/DGAT) which is a bifunctional acyltransferase involved in TAG and wax ester synthesis in oleaginous microorganisms (2) and typically accumulate polyhydroxybutyrate (PHB) as storage materials of carbon and energy (3, 4). Nevertheless, the accumulation of neutral lipids and/or lipid droplets in cyanobacterial cells has been repeatedly reported in literature. In a wide range of species, such as *Nostoc commune* (5), *Arthrospira platensis* (6), *Nostoc punctiforme* (7), *Synechocystis* sp. PCC 6803 (8), *Calothrix* sp. 336/3, *Microcystis* sp., *Synechococcus* sp., and *Snowella litoralis* (9), the accumulation of TAG has been identified by thin-layer chromatography (TLC) based on the mobility similar to the TAG standards. In some

Competing Interest: The authors declare no competing interest.
Received: December 15, 2022. **Accepted:** March 13, 2023

studies, the excised spots were further analyzed by gas chromatography–mass spectrometry (GC–MS) and the composition of the detected fatty acids was reported (7, 8). However, whether these fatty acids were really derived from TAG molecules or not remained uncertain due to methanolysis of the samples before GC–MS analysis.

In the previous report, we separated the neutral lipids of the wild-type (WT) cells of *Synechocystis* sp. PCC 6803 (hereafter S.6803) by TLC and analyzed the components within the spot showing the TAG-like mobility (hereafter TAG-like spot) by liquid chromatography–tandem mass spectrometry (LC–MS/MS) without methanolysis (10). Unexpectedly, the amount of TAG within the TAG-like spot was only one-tenth of that was expected from the amount of fatty acids quantified by GC analysis, which means that the major component of the TAG-like spot in S.6803 is not TAG but unknown lipid molecule(s) containing fatty acids. Moreover, we found that the TAG-like spot was not detected in the gene-disrupted strain of *slr2103* having homology with the eukaryotic diacylglycerol acyltransferase-2 (DGAT2) gene family. Independent of our study, Aizouq et al. (11) reported the absence of the TAG-like spot in the deletion mutant of *slr2103*. They concluded that Slr2103 is involved in TAG and fatty acid phytyl ester synthesis in S.6803 based on the mutant analysis and acyltransferase assay of the Slr2103 recombinant protein. However, the accumulation level of phytyl esters in the WT cells was quite low in the study, and whether phytyl esters are the component of the TAG-like spot has not been assessed. Thus, the main product of Slr2103 in S.6803 cells, which possibly is the main component of the TAG-like spot, remains to be elucidated.

This study resolves the abovementioned long-standing questions about the accumulation of neutral lipids in cyanobacteria. We successfully identify monoacylated derivatives of plastoquinol (PQH_2) as the physiological product of Slr2103 and as the predominant molecular species in the TAG-like spot in not only S.6803 but also *N. punctiforme* PCC 73102 (hereafter *N. punctiforme*) and *Anabaena* sp. PCC 7120 (hereafter A.7120). Although borondipyrromethene difluoride (BODIPY) fluorescence signals were detected within these cells as reported previously, the typical lipid droplet structures were never observed. Aggregates of lipophilic materials consisting of alkane, free C16 and C18 saturated fatty acids, and low amounts of TAG are likely to accumulate in the cytoplasmic area and be stained by BODIPY, whereas acyl PQH localizes exclusively in the membrane fraction.

Results

Conservation of DGAT2-like proteins in cyanobacteria

The overall amino acid sequence of Slr2103 exhibits similarity to the DAGAT domain (Pfam PF03982), which is highly conserved among eukaryotic DGAT2 family enzymes. In contrast to the absence of the bacterial TAG-synthesizing enzyme WS/DGAT in cyanobacteria, DGAT2-like proteins are broadly distributed across the phylum. We searched genes encoding DGAT2-like proteins from 126 cyanobacterial genome sequences (12) and obtained 102 sequences. Phylogenetic analysis revealed that their amino acid sequences diverge into 2 distinct subclades, clade A (85 sequences) and clade B (17 sequences), both of which are clearly separated from the eukaryotic DGAT2 clade (Fig. 1). As shown in Fig. S1, some of the deep-branching lineages and marine picocyanobacterial having the streamlined genomes do not possess DGAT2-like proteins. The other species tend to have at least 1 clade A copy, indicating the physiological importance of DGAT2-like proteins for cyanobacteria. Interestingly, 11 out of 17 species having clade B copies belong to the order *Nostocales*, the filamentous heterocyst-forming genera repeatedly reported to accumulate TAG and/or lipid body. The species used in this study, *N. punctiforme*, possesses Npun_R5090 (clade B) as well as Npun_F6258 (clade A), and A.7120 possesses Alr0790 (clade B) in addition to 2 clade A copies, Alr0981 and Alr1233.

Generation of the ox-*2103* strain and detection of the TAG-like spot

In the previous study, we found that the TAG-like spot was not detected in the *slr2103*-disrupted strain (Δ*2103*) in S.6803 (10). Here, we made the overexpression strain of *slr2103* (ox-*2103*) to further characterize the product of Slr2103 responsible for the TAG-like spot. The *slr2103* gene fused to the strong *psbA2* promoter was introduced into the neutral site of the S.6803 genome (the *slr2031* region) together with the kanamycin-resistance cassette (Fig. S2A). The complete segregation of the resultant strain was verified by PCR amplification of the *slr2031* region (Fig. S2B).

To evaluate the amount of the unknown neutral lipid produced by Slr2103 and its commonality among the cyanobacterial species, total lipid was extracted from the Δ*2103*, WT, and ox-*2103* strains of S.6803, as well as WT strains of *N. punctiforme* and A.7120 grown under high light (HL) conditions for 7 days. When neutral lipids extracted from cells with the same dry weight (DW) were separated on a silica gel TLC (Fig. 2A), a TAG-like spot showing slightly different mobility compared with TAG standard was detected in S.6803 WT but not in Δ*2103* as reported previously (10). The intensity of the TAG-like spot was higher in ox-*2103* than that in WT, supporting that Slr2103 is responsible for the synthesis of the unidentified neutral lipid. In *N. punctiforme* and A.7120, the TAG-like spots were detected with much higher intensities than that in ox-*2103*, reflecting the known characteristic of *Nostocales*, which is rich in neutral lipids.

Chemical characterization of the predominant neutral lipid species in the TAG-like spot

The TAG-like spot of ox-*2103* was excised from the TLC plate, and lipid components were analyzed by gas chromatograph–mass spectrometry (GC–MS) after methanolysis and trimethylsilyl (TMS) derivatization (Fig. S3). Fatty acids 16:0 and 18:0 were the predominant components in the fraction as reported in Tanaka et al. (10), and 17:0, 18:1, 18:2, and 18:3 fatty acids were detected as the minor components. However, the TMS derivative of phytol was never detected, indicating that the TAG-like spot does not contain phytyl esters, one of the potential products of Slr2103 reported by Aizouq et al. (11).

To further address the molecular structure of the neutral lipid species in the TAG-like spot, the fraction without methanolysis was analyzed by reverse-phase LC–MS with an electron spray ionization (ESI). In the 20–30 min of elution time corresponding to highly hydrophobic eluents, two major peaks were detected both in positive and negative ionization modes (P1 and P2 shown in Fig. 2B). In the MS spectrum of the highest peak P1 in positive mode, the *m/z* 989.9, 1006.9, 1011.9, and 1027.9 were detected, which were estimated as adduct ions of M = 988.9 with H^+, NH_4^+, Na^+, and K^+, respectively (Fig. 2C). The negative mode gave a simpler MS spectrum with *m/z* 987.9 and the isotopic ions, which was estimated as $(M–H)^-$. The MS spectrum of the second major peak P2 showed the same pattern with an increment of *m/z* 28 than those of P1, indicating a longer chain of fatty acid by 2 carbons. From these MS spectra together with the fatty acid profile

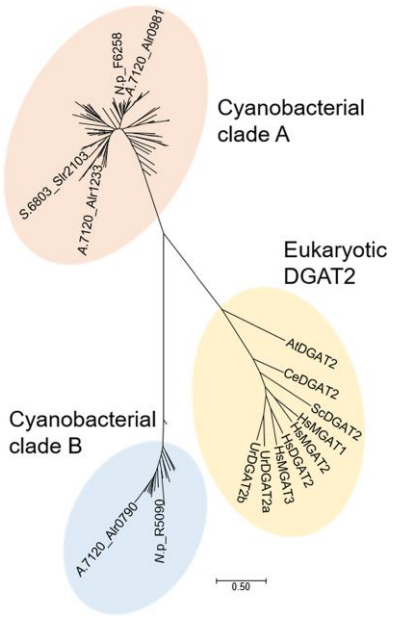

Fig. 1. The unrooted dendrogram depicting the evolutionary relationship of the eukaryotic DGAT2 and cyanobacterial DGAT2-like proteins. A total of 102 amino acid sequences of cyanobacterial DGAT2-like proteins were diverged into 2 distinct subclades. Only the names of Slr2103 from S.6803, Npun_F6258 and Npun_R5090 from *Nostoc punctiforme* PCC 73102 (*N. punctiforme*), and Alr0981, Alr1233, and Alr0790 from *Anabaena* sp. PCC7120 (A.7120) are indicated. As representatives of proteins belonging to the eukaryotic DGAT2 family, DGAT2 and 3 acyl-CoA: monoacylglycerol acyltransferases (MGATs) from *Homo sapiens* (Hs), DGAT2a and DGAT2b from *Umbelopsis ramanniana* (Ur), and DGAT2 from *Caenorhabditis elegans* (Ce), *Saccharomyces cerevisiae* (Sc), and *Arabidopsis thaliana* (At) are presented. Phylogenetic analysis was performed using the MEGA7 software based on the maximum likelihood method.

obtained by GC–MS (Fig. S3), the molecular weights of the two major peaks P1 and P2 were estimated as 988.9 and 1016.9, which contain a 16:0 and 18:0 fatty acyl moiety, respectively. The molecular weights are significantly larger than TAG (up to 909) (10) or phytyl esters (up to 563) (11), suggesting that TAG-like spot contains a novel fatty acyl derivative with a very large molecular weight.

We then attempted basic chemical treatments of the unidentified lipid in the TAG-like spot to estimate its structure. Mild alkaline hydrolysis of the TLC fraction resulted in the complete loss of the LC–MS peaks (Fig. S4), suggesting that the substances were fatty acyl esters and that the alcoholic moiety bound to fatty acids was undetectable under the LC–ESI–MS condition. Acetylation with acetic anhydride provided a change in the LC–MS profile (Fig. 2D). Some of the peaks showed no changes in the retention time of MS spectrum. For example, the extracted ion chromatogram (EIC) clearly showed that *m/z* 824.7 of peak 2 in Fig. 2D was unchanged by acetylation (Fig. S5A). This *m/z* accorded with TAG with tripalmitate (48:0, ammonium adduct). Similarly, peaks 4, 7, and 9 were not affected by acetylation and assigned to TAG 50:0, 52:0, and 54:0, respectively. On the other hand, there were peaks that showed the shift of both *m/z* and retention time. EIC at *m/z* 1006.9 gave peak 5 (same as P1 in Fig. 2B) but disappeared after acetylation (Fig. S5B). Instead, the single peak of *m/z* 1048.9 newly emerged at a slightly longer retention time (Fig. S5C),

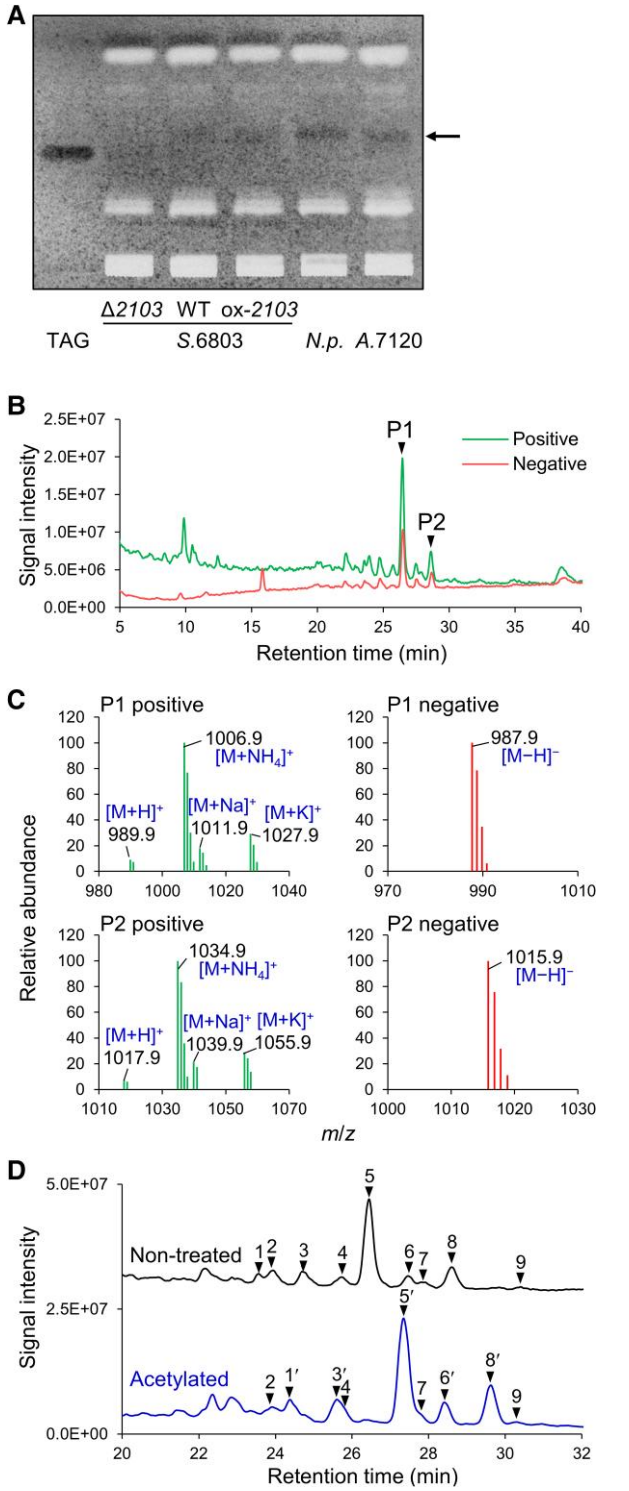

Fig. 2. TLC separation and LC–MS characterization of neutral lipids from cyanobacteria. A) Neutral lipids from the cyanobacteria and TAG standard were separated by TLC. The TAG-like spot shown by an arrow was collected for further characterization. Each lane contains the lipid extracts from cells with the same DW (10-mg DW). B) LC–MS chromatograms of lipid components in the TAG-like spot from ox-*2103* were obtained with positive and negative ionization modes. C) Major MS spectra of the 2 major peaks P1 and P2. D) LC–MS chromatogram of pre- and postacetylation. (See Table S1 for identification of the peaks based on the MS spectra.)

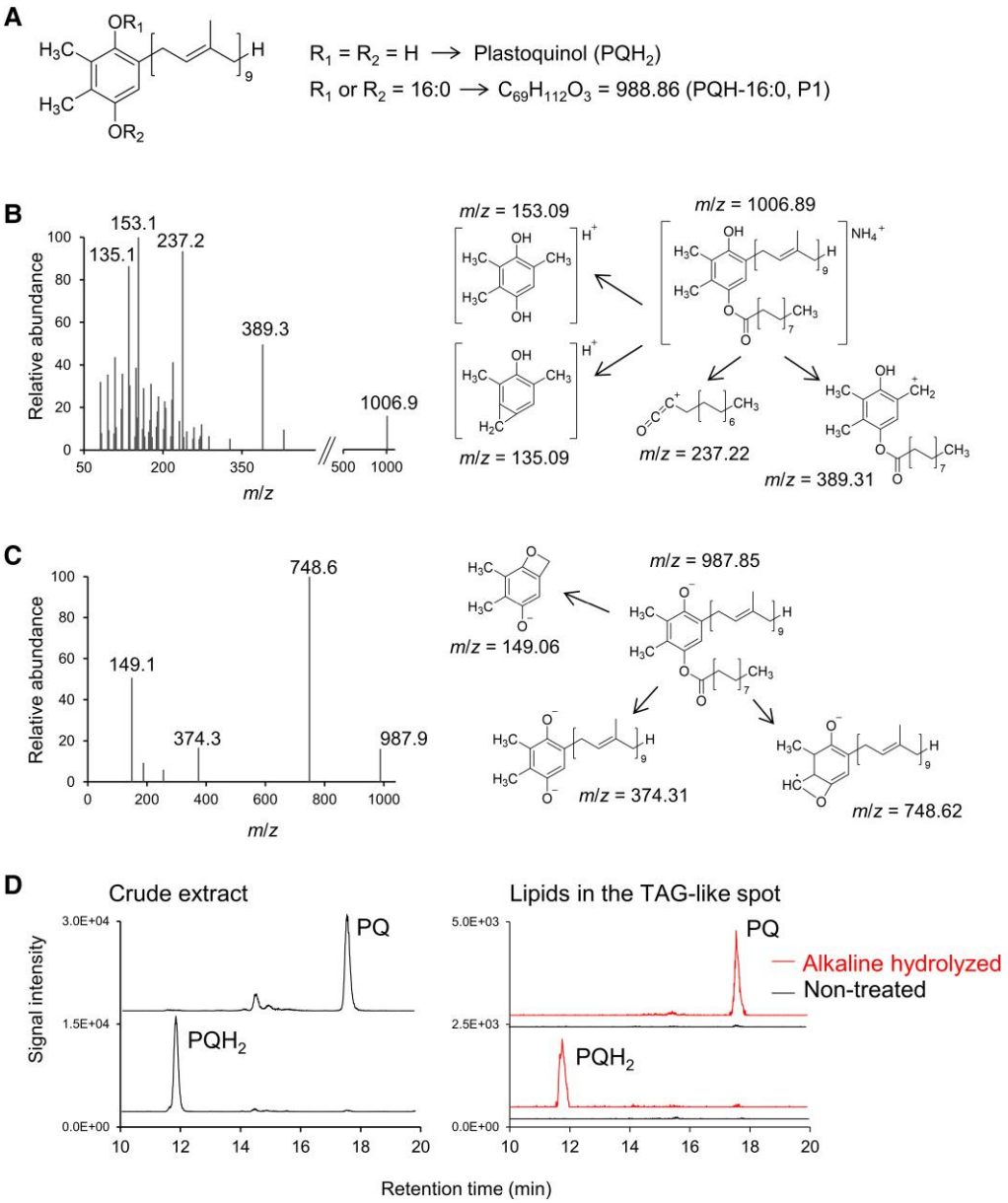

Fig. 3. Assignment of MS/MS spectra to acyl PQH. A) The structure and theoretical mass of *O*-acyl plastoquinol. MS/MS spectra obtained by the positive (B) or negative (C) mode of the unidentified lipid (P1) were assigned to the estimated fragmentation products of PQH-16:0 (R2-acylated form shown). D) Crude extract of S.6803 WT (control for free quinone detection) and the hydrolysate of the lipids in the TAG-like spot were analyzed by LC–APCI–MS/MS for PQ (*m/z* 749 > 151) and PQH_2 (*m/z* 751 > 151).

indicating that the molecule of the peak 5 underwent monoacetylation with Δ42 increase of the mass. The similar shifts of *m/z* and elution time were also found in the peaks 1, 3, 6, and 8, and their *m/z* differences indicated the series of fatty acyl moieties as detected in GC–MS (Table S1).

Structural identification of the predominant neutral lipid species in the TAG-like spot

The results described above demonstrated that the unidentified lipid in the TAG-like spot contains a fatty acyl chain and a free hydroxy group, resulting in a large mass ~1,000. As the most reasonable molecule that well explains the data obtained, we here propose the monoacylated derivative of plastoquinol (PQH_2). PQH_2 is the reduced form of plastoquinone (PQ) which is commonly present in the thylakoid membranes as an electron transfer component, and the theoretical mass of its monoacylated form (acyl PQH) is identical to the detected mass of the unidentified lipid (Fig. 3A). To validate this hypothesized structure, we further analyzed by LC–ESI–MS/MS. In the positive ionization mode, many product ions were detected through collision-induced fragmentation of the precursor ion *m/z* 1006.9 (peak 5 in Fig. 2D), and the major signals were successfully assigned to the estimated fragments derived from mono-palmitate derivative of PQH_2 (PQH-16:0; Fig. 3B). Several fragments seem to be produced by losing the 9 isoprenyl units from the methylquinone moiety, which is similar to the fragmentation pattern recently reported for free PQH_2 and PQ in an atmospheric pressure chemical ionization (APCI)-coupled LC–MS/MS analysis (13). A similar result was obtained in *m/z* 1034.9 (peak 8 in Fig. 2D) with the increments of

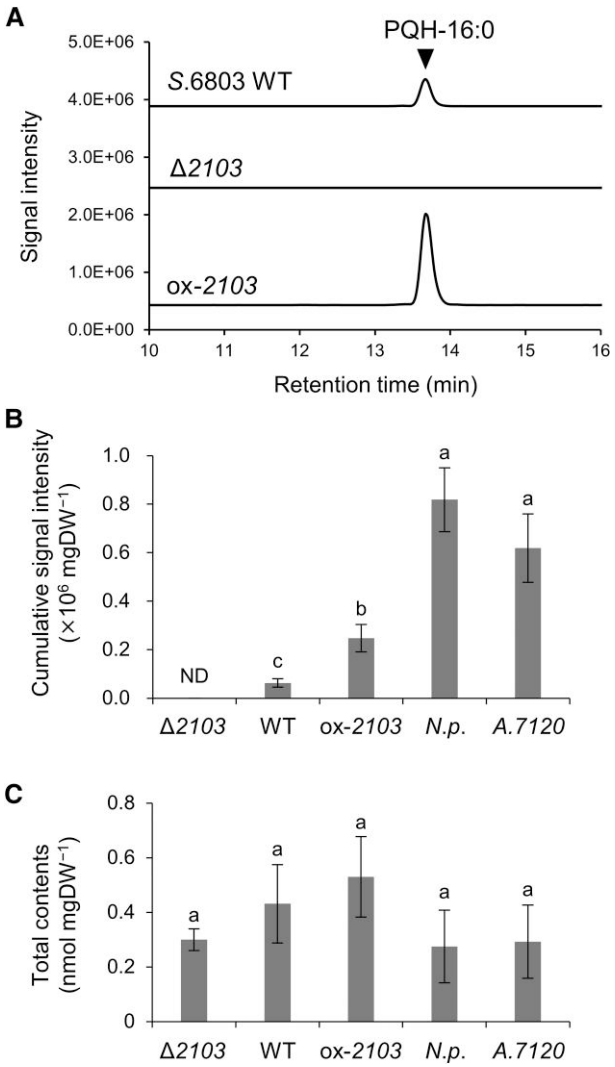

Fig. 4. Quantification of acyl PQH and TAG. A) LC–MS/MS chromatograms of PQH-16:0 from S.6803 WT, Δ2103, and ox-2103. B) Acyl PQH level was assessed by signal intensity. C) TAG level was expressed as nmol using a standard. Quantitative values were normalized with dry weight (DW) of each sample. Data are mean ± SD ($n = 3$), and different letters on bars indicate statistical significance (Tukey–Kramer test, $P < 0.05$). ND, not detected.

m/z by 28 for the fragments containing the fatty acyl moiety but not for those from the quinone moiety, indicating the presence of 18:0 in place of 16:0. The negative MS/MS analysis provided *m/z* 748.6 and 374.3 that corresponded with the monovalent and divalent ions of the plastoquinol moiety produced by the loss of the fatty acyl chain (Fig. 3C). These MS/MS spectra supported the estimated structures of the unidentified lipid in the TAG-like spot. The results of the acetylation experiment suggest one of the two free hydroxy groups of quinone remains free, which excludes the possibility of plastochromanol-8, the circulated isomer of PQH_2 with only one free hydroxy group (14). It should be noted that we could not determine which the hydroxy group of PQH_2 is esterified.

The ^{1}H-nuclear magnetic resonance (NMR) analysis of the lipid components in the TAG-like spot also supported the structure of monoacylated PQH (Fig. S6). The ^{1}H-NMR signals corresponding to the substituents of the partial structure contained in TAG were observed in the normal regions, respectively, as shown in Fig. S6. The 1D ^{1}H-NMR spectrum showed the complicated signals between broad regions of 1.0 to 2.2, 3.1 to 3.5, 4.6 to 5.5, and 7.0 to 7.2 ppm, which contained the chemical shifts assigned to not only the fatty acyl moiety (αCH_2, βCH_2, and other CH_2) but also the methylquinol and isoprenyl moieties of PQH (Fig. S6A). These assignments were also supported by the 2D ^{1}H-^{1}H correlation spectroscopy (COSY) spectra (Fig. S6B).

Finally, the lipid components in the TAG-like spot were alkaline-hydrolyzed and analyzed by LC–APCI–MS/MS to evaluate whether free PQH_2 was liberated or not (Fig. 3D). As the control experiment, free PQH_2 and PQ in the crude extract of S.6803 WT were detected using the method described for eukaryotic algae (13). The signals of PQH_2 and PQ were not detected in the nontreated sample but arose after alkaline hydrolysis, which evidenced the presence of the PQ moiety in the unidentified lipid in the TAG-like spot.

Accumulation level of the acyl PQH and TAG species in cyanobacterial cells

The above analyses to determine the molecular structure of the unidentified lipid together with the previous observations (10) indicated that the TAG-like spot in S.6803 contains acyl PQH as the main component and lesser amounts of TAG. To compare the accumulation level of acyl PQH and TAG among different cyanobacterial strains with various TAG-like spot intensity (Fig. 2A), we developed LC–MS/MS-targeted analysis for simultaneous detection of the acyl PQH and TAG species. Figure S7 shows LC–MS/MS chromatograms with the multiple reaction monitoring (MRM) for each lipid species. A series of acyl PQH and TAG with various fatty acyl moieties was selectively detected as single peaks by the C18 reverse-phase LC–ESI–MS/MS. When this method was applied to the TLC-purified fractions prepared from S.6803 WT, Δ2103, and ox-2103 with the same cell dry weight (CDW), the PQH-16:0 signal absolutely disappeared in Δ2103, whereas the signal intensity was significantly higher in ox-2103 than that in WT (Fig. 4A). Similar results were obtained for other acyl PQH species. We quantified the peak intensities of the triplicated data by normalization with the CDW (Fig. 4B). As expected from the raw chromatograms, the obtained result showed the loss and 4.2-times increase of total acyl PQH levels in Δ2103 and ox-2103, respectively. On the other hand, TAG contents were comparable among the strains (Fig. 4C). These results confirmed that Slr2103 is responsible for generation of acyl PQH but not TAG in S.6803, and acyl PQH is the major component of the TAG-like spot observed in TLC analysis. When the same quantitative analysis was performed on *N. punctiforme* and A.7120, they showed >2-times higher level of acyl PQH than ox-2103, but comparable or lower level of TAG compared with the S.6803 strains (Fig. 4). There was correlation between the TAG-like spot intensities (Fig. 2A) and MS-determined levels of acyl PQH in every strain. These observations strongly suggest that the main component of the TAG-like spot in *Nostocales* species is also acyl PQH but not TAG.

The fatty acid profiles of acyl PQH and TAG were similar in that they were abundant in saturated 16:0 and 18:0 but poor in polyunsaturated fatty acids (Fig. S8), suggesting that de novo-synthesized fatty acids rather than membrane lipid catabolites are incorporated into these neutral lipids. It is worth noting that 17:0, unusual fatty acid in cyanobacteria but slightly detected by GC–MS in the TAG-like spot (Fig. S3), was abundantly detected in acyl PQH except for A.7120. On the other hand, 18:1 which

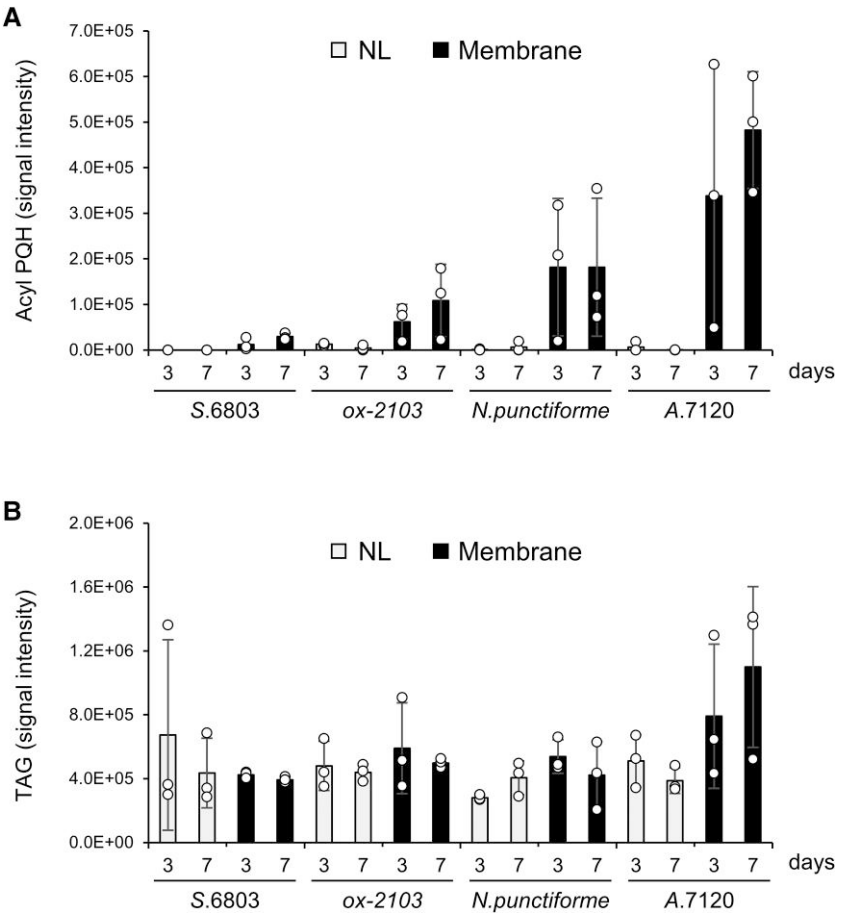

Fig. 5. Quantification of A) acyl PQH and B) TAG in the neutral lipid-enriched (NL) and membrane fractions. The TAG-like spots in the NL and membrane fractions prepared from 3- and 7-day cultures were excised from the TLC plate, and acyl PQH and TAG were quantified by LC–MS/MS. Data are mean ± SD ($n = 3$).

was one of the major components of TAG was hardly detected in acyl PQH.

Microscopic observation of the accumulation of neutral lipids in cyanobacterial cells

The coexistence of TAG and acyl PQH in S.6803 and *Nostocales* species has raised a new question concerning the intracellular localization of these neutral lipids. In S.6803 and *N. punctiforme*, there have been some studies reporting the accumulation of neutral lipid droplets visualized microscopically using the green fluorescent dye BODIPY, which specifically stains neutral lipids. Hauf et al. (8) observed that some S.6803 WT cells at the early exponential phase of growth showed strong intracellular fluorescence signals. TLC spots showing the TAG-like mobility were detected from these cells. In the case of *N. punctiforme*, most cells showed prominent fluorescence signals at the stationary phase of growth (7, 15) and the lipid droplet-enriched fraction was reported to contain α-tocopherol, TAGs containing C16:0 and C18:0 fatty acids, and C17 alkanes (7). Since identification of TAG was based on the TLC mobility similar to the TAG standards, it remained to be determined whether either or both TAG and acyl PQH is included in the lipid droplets.

In order to examine whether lipid droplet-like structures which had been reported in literature could be observed in cyanobacterial strains used in this study, we stained the Δ*2103*, WT, and ox-*2103* strains of S.6803 and WT strains of *N. punctiforme* and A.7120 grown under HL conditions for 3 or 7 days with the BODIPY dye (Figs. S9 and S10). In S.6803 WT and Δ*2103*, BODIPY fluorescence signals similar to those reported by Hauf et al. (8) became prominent in 7 days. In these cells, a few particles often occupied >10% of cell area. It is notable that an increase of BODIPY fluorescence during HL incubation was hardly observed in ox-*2103*. In *N. punctiforme* and A.7120, multiple particles of BODIPY fluorescence were detected as reported by Peramuna and Summers (7). Due to the large cell size of *Nostocales* species, the area of BODIPY fluorescence per cell seldom exceeded 10%. The accumulation was already obvious in 3 days in A.7120, whereas a large increase was observed by 7 days in *N. punctiforme*. In every strain, the diameter of lipid droplet-like structures was ~300 nm, which is consistent with the observation by Peramuna and Summers (7).

Next, we performed transmission electron microscopy (TEM) analysis (Figs. S11 and S12) on the same cyanobacterial cultures that were used for BODIPY staining (Figs. S9 and S10) to assess whether BODIPY fluorescence detected in these samples was indeed originated from lipid droplets. In S.6803 cells, typical intracellular organization was observed regardless of the sampling time and strains. Namely, a central cytoplasmic area containing carboxysomes was surrounded by concentric layers of thylakoid membranes (Fig. S11). In the thylakoid membrane region, several large electron-transparent PHB granules, electron-dense lipid droplets, and numerous small glycogen granules were observed.

As reported previously in the unicellular cyanobacterial species (16–19), lipid droplets with an average diameter of 50–100 nm (denoted as "L" in Fig. S11A) were localized in the cell periphery, in the close vicinity of both thylakoid and cytoplasmic membranes. Δ*2103* contained less lipid droplets compared with WT, whereas the distinctive mesh-like structure of thylakoid membranes filled with electron-dense particles was observed only in the ox-*2103* cells (Fig. S11B). These lipid droplets and small electron-dense particles were not detected as BODIPY fluorescence. Rather, the size, localization, and the number within each cell of PHB granules (denoted as "P" in Fig. S11A) coincided well with those of BODIPY fluorescence (Figs. S10 and S11A). As expected from the results of BODIPY staining (Figs. S10 and S11A), ox-*2103* contained less PHB granules compared with WT and Δ*2103* (Fig. S11A).

In *N. punctiforme*, the concentric layers of thylakoid membranes observed in the 3-day sample were totally disappeared in the 7-day sample and every cell within the filaments became spherically enlarged (Fig. S12). Carboxysomes were detected in the central cytoplasmic area, whereas small electron-transparent particles were accumulated in the peripheral area, where typical thylakoid organization had been observed in 3 days. The localization of these particles did not coincide with that of BODIPY fluorescence which was detected mainly in the central cytoplasmic area. In *A.*7120, the heterogeneity in the ultrastructure of individual filaments was obvious both in the 3-day and 7-day samples. Some remained structurally intact, but the others consisted of swollen cells in which the interthylakoid space was significantly enlarged and filled with electron-transparent materials. Although the electron-dense cyanophycin granules were characteristically observed in the 7-day sample, lipid droplet-like structures or PHB granules which could be stained by BODIPY were not observed.

Localization of the acyl PQH and TAG species in cyanobacterial cells

In order to examine the localization and abundance of TAG and acyl PQH in the abovementioned strains grown under HL for 3 or 7 days, the neutral lipid-enriched fraction (NL fraction) was isolated from the crude lysates of cells with the same DW by sucrose density gradient centrifugation using the previously reported method (7, 10). After the first ultracentrifugation, the orange layer on the top of the sucrose gradient and the ultracentrifuge pellet were collected as the NL fraction and the membrane fraction, respectively (Fig. S13A). Although it is unclear whether the NL fraction is concentrates of the "lipid droplets" detected as BODIPY fluorescence signals within cyanobacterial cells, it contains numeral small particles that can be stained by BODIPY (7, 10). After further purification of the NL fraction by the second ultracentrifugation, lipids were extracted from each fraction and loaded onto TLC plates. Figure S13B shows the results of the separation of neutral lipids in biological triplicate. In every strain, the TAG-like spot containing acyl PQH and/or TAG was detected both in the NL and membrane fractions and the spot intensity was unchanged during HL incubation. There were several other spots in the NL fraction. Alkane detected as high mobility spots near the solvent front (7, 10) became more prominent in the NL fraction after 7 days. The spot with lower mobility than TAG standard was analyzed by LC–MS/MS and assigned to be free fatty acids. The free fatty acids detected in the NL fraction were enriched in saturated species, whereas small amounts of unsaturated free fatty acids were detected in the membrane fraction (Table S2). It is notable that unsaturated free fatty acids were highly accumulated in the membrane fraction of *A.*7120 (Fig. S13 and Table S2).

The TAG-like spots were excised from the TLC plate, and acyl PQH and TAG contained in the NL and membrane fractions were quantified by LC–MS/MS (Fig. 5). In every strain, acyl PQH was exclusively localized in the membrane fraction, whereas TAG was detected at similar levels in both NL and membrane fractions. The accumulation level of both neutral lipids was not significantly changed during HL incubation.

Discussion

In this study, we determined that acyl PQH is the major component of the TLC spot showing TAG like mobility and is the physiological product of Slr2103 belonging to clade A of cyanobacterial DGAT2-like proteins. Independently of our study, Mori-Moriyama et al. (20) have identified that acyl PQH is the major component of the TAG-like spot in *Synechocystis* sp. PCC 6803 and *Nostoc punctiforme* PCC 73102 (20). They purified acyl PQH using two-dimensional thin-layer chromatography and determined its structure mainly using ^{1}H and ^{13}C NMR. The appropriateness of the structure is strongly supported by the fact that two groups obtained the same structure by using different identification methods.

The accumulation level of acyl PQH (Fig. 4B) was well correlated with the intensity of the TAG-like spot (Fig. 2A) in every strain examined and with the expression level of *slr2103* among Δ2103, WT, and ox-*2103* strains of *S.*6803. On the other hand, we could not obtain data supporting the notion that TAG and phytyl esters are physiological products of Slr2103 (11). Namely, the accumulation level of TAG was not affected by deletion or overexpression of *slr2103* (Figs. 4C and 5B) and phytyl esters were not detected as far as we investigated.

As exemplified by DGAT2 and monoacylglycerol acyltransferase (MGAT) both included in the eukaryotic DGAT2 clade (Fig. 1), the eukaryotic DGAT2 family has arisen by gene duplication and evolved to catalyze the synthesis of distinct lipids (21). It is no wonder that clade A cyanobacterial DGAT2-like proteins evolved to exhibit acyltransferase activity toward PQH_2 which is abundantly present in the thylakoid membranes. The physiological role of acyl PQH production remains unknown, since growth property was not affected by the disruption of *slr2103* under various growth conditions (10). Our data suggest that the fairly constant level of acyl PQH is synthesized and accumulated within the membrane fraction (Fig. 5A) irrespective of light intensity and nutrient availability (10). In analogy with synthesis of fatty acid phytyl esters in plant plastoglobules (22), the excess amount of fatty acyl moieties and PQH_2 within thylakoid membranes may be incorporated into acyl PQH for the safe storage. In nitrogen-deprived plants, a coordinated breakdown of galactolipids and chlorophylls results in the accumulation of the specific fatty acid phytyl esters, 16:3-phytol (23). In the case of acyl PQH in cyanobacteria, the incorporation of fatty acyl moieties released from membrane lipids is not likely, since the predominant fatty acyl moieties of acyl PQH are 16:0 and 18:0 in every strain examined (Fig. S8). There may exist constitutive activity of DGAT2-like enzymes esterifying de novo-synthesized fatty acids to PQH_2. High conservation of clade A of DGAT2-like proteins indicates the importance of such activity for cyanobacteria (Fig. S1).

In *S.*6803 cells, lipid droplets with an average diameter of 50–100 nm (denoted as "L" in Fig. S11A) were observed between the thylakoid membrane pairs and adjacent to the cytoplasmic membrane, as reported in literature (16–19). The number of these

droplets decreased by the disruption of *slr2103*, which is consistent with the observation by Aizouq et al. (11). On the other hand, mesh-like structure of thylakoid membranes filled with electron-dense particles was specifically observed in ox-*2103* (Fig. S11B). These observations imply that these droplets and structures are derived from Slr2103 activity. Concerning their composition, there are two possibilities, acyl PQH and other unidentified lipid species produced by Slr2103. In the former case, these droplets and structures must be coprecipitated with thylakoid membranes, since acyl PQH was exclusively detected in the membrane fraction (Fig. 5A). In the latter case, the unidentified product of Slr2103 should be detected by TLC of neutral lipids (Fig. S13B) especially in ox-*2103*. However, we detected no significant spot other than alkane, TAG/acyl PQH, and free fatty acids in both NL and membrane fractions. Further analyses are needed to clarify the nature of these structures that may be produced by Slr2103.

We reported in the previous study that the accumulation level of TAG in S.6803 WT cells was higher than the background noise contamination, but they accounted for only 10% of the neutral lipid contained in the TAG-like spot (10). In this study, we found that *Nostocales* species accumulated similarly low levels of TAG (Fig. 4C and Fig. 5B). As is the case with acyl PQH, the predominant acyl moieties of TAG are 16:0 and 18:0, indicating that de novo-synthesized fatty acids are the main source of TAG synthesis. Since 17:0 and 18:1 were selectively contained in acyl PQH and TAG, respectively (Fig. S8), acyl PQH and TAG are synthesized, in part, via different fatty acid resources and/or by enzymes different in the preferences of fatty acid substrates. TAG-synthesizing activity in S.6803 may be due to acyltransferases with broad substrate specificity other than Slr2103, whereas that in *Nostocales* species may be due to DGAT2-like proteins belonging to clade B.

Microscopic observation together with lipid analyses of cyanobacterial cells incubated under HL conditions revealed the commonalities and differences in the accumulation of neutral lipids between cyanobacterial species. One of the commonalities is the accumulation of BODIPY fluorescence during HL incubation. However, when cellular ultrastructure was observed by TEM, qualitative difference was significant between S.6803 and *Nostocales* species. In S.6803, the concentric layers of thylakoid membranes were not affected by HL incubation and increase of BODIPY fluorescence was likely to reflect the accumulation of PHB granules (Fig. S11). PHB granules have been reported to accumulate in S.6803 cells at stationary phase (24) and be stained by dyes for neutral lipids such as Nile red and BODIPY (4, 25, 26). In S.6803 at the early exponential phase of growth, transient appearance of strong BODIPY fluorescence signals was reported (8). The authors discussed that this is due to the accumulation of lipid droplets working as a dynamic reservoir for fatty acid storage and turnover. Thus, BODIPY fluorescence could be observed within S.6803 cells either at the early exponential phase or at the stationary phase, reflecting the accumulation of the different compounds, fatty acids, or PHB granules. The accumulation level of these lipophilic compounds is largely affected by cellular metabolic status. In our study, the accumulation of BODIPY fluorescence was hardly observed after 7 days of HL incubation in ox-*2103* (Figs. S9 and S10). This may be the consequence of redirection of carbon flux toward acyl PQH synthesis. Hauf et al. (8) reported that TAG-like spot in WT mainly contained 16:0 and 18:0, with low amount of 15:0 and 17:0, which coincides with the fatty acid composition of acyl PQH (Fig. S8). In the PII mutant, the additional spot was observed right above the TAG-like spot observed in WT. This spot contained 16:0 and 18:0, but not 15:0 and 17:0, which coincides with the fatty acid composition of TAG (Fig. S8). It is likely that TAG as well as acyl PQH is accumulated in the PII mutant lacking control of acetyl-CoA carboxylase activity.

There have been some reports of TAG accumulation in the order *Nostocales* (5, 7, 27). However, none of these studies examined the ultrastructure of "TAG"-accumulating cells by using TEM and it remained unknown whether these cells accumulate lipid droplets like oleaginous bacteria such as *Rhodococcus*. In this study, we clearly show that *N. punctiforme* and A.7120 cells exhibiting prominent BODIPY fluorescence signals after 7 days of HL incubation do not contain typical lipid droplet structures enclosed by a lipid monolayer (Fig. S12). In these cells, profound rearrangement or disappearance of the thylakoid structure together with the accumulation of electron-transparent unstructured particles was observed. Although there is possibility that these particles are filled with lipophilic material, their shape, size, and localization did not always coincide with those of BODIPY fluorescence.

Therefore, NL fraction obtained by ultracentrifugation in this study cannot be considered as the lipid droplet fraction but the concentrates of lipophilic materials accumulated in the cytoplasmic area. TLC analysis revealed that the composition of neutral lipids is quite similar among S.6803, *N. punctiforme*, and A.7120 cells (Fig. S13). Namely, spots of alkane and free fatty acids were detected more prominently than TAG-like spots. TAG-like spots in the NL fraction can be regarded as the concentrated TAG fraction, since acyl PQH is not contained in the NL fraction as shown by LC–MS/MS analysis (Fig. 5A). Taken together, the accumulation level of TAG in the cytoplasmic area must be much lower than that of alkane and free fatty acids. Peramuna and Summers (7) reported that NL fraction of *N. punctiforme* was enriched for C17 alkane, α-tocopherol, and TAG containing only C16:0 and C18:0 fatty acids. Considering that they did not detect C17:0 from the TAG-like spot, TAG but not acyl PQH must be contained also in their NL fraction. Although the effect of cultivation under HL for 7 days on the thylakoid membrane structures differed significantly among S.6803, *N. punctiforme*, and A.7120 cells (Figs. S11 and S12), the composition of neutral lipids in the membrane fraction was quite similar among them, except for high accumulation of free fatty acids in A.7120 cells (Fig. S13B). LC–MS/MS analysis revealed that the TAG-like spot from the membrane fraction contains both acyl PQH and TAG (Fig. 5). A slight difference in the mobility of the TAG-like spot between the NL and membrane fraction (Fig. S13B) may reflect the presence or absence of acyl PQH in the spot.

In conclusion, our study provides answers to long-standing questions about the accumulation of neutral lipids in cyanobacteria. As expected from the lack of the bacterial TAG-synthesizing enzyme WS/DGAT, cyanobacteria do not accumulate lipid droplet structures such as those observed in oleaginous microorganisms. Instead, they accumulate PHB granules or aggregates of lipophilic materials in the cytoplasmic area, which can be detected as BODIPY fluorescence signals. The lipophilic materials consist of alkane, free C16 and C18 saturated fatty acids, and low amounts of TAG. In addition, there are acyl PQH and low amounts of TAG accumulating in membrane fractions, which have been detected by TLC as TAG-like spots. Most of these neutral lipids are synthesized using de novo-synthesized fatty acids rather than those released from membrane lipids. Clade A of cyanobacterial DGAT2-like proteins is responsible for acyl PQH synthesis, whereas the function of clade B proteins remains to be elucidated. As far as we know, this is the first study to show the physiological role of DGAT2-like proteins widely distributed among bacterial phyla. In contrast to the extensively studied eukaryotic DGAT2 family proteins, bacterial

DGAT2-like proteins have received little attention. Further studies on cyanobacterial DGAT2-like proteins may pave the way for the elucidation of the origin and evolution of DGAT2 family proteins.

Materials and methods

Generation of the ox-2103 strain

The pTKP2031 vector containing the kanamycin-resistance cassette and the strong *psbA2* (*slr1311*) promoter flanked by a part of the coding regions of *slr2030* and *slr2031* as a platform for homologous recombination (28) was linearized by inverse PCR using the primer pair of HpaI-2031-F and PpsbA-R (Table S3) for cloning of the *slr2103* gene into the NdeI/HpaI site of the vector. The coding sequence of the *slr2031* gene (nucleotide from 1571731 to 1572615 according to the numbering in CyanoBase) was amplified by PCR using the primer pair of PpsbA-slr2103-F and 2031-slr2103-R (Table S3). The linearized pTKP2031 vector and the *slr2103* gene were fused using the In-Fusion HD Cloning Kit (Clontech, USA) to generate pTKP2031-*slr2103* construct. The construct was transformed into the glucose-tolerant WT strain of S.6803 to yield the ox-*2103* strain having insertion of the *PpsbA-slr2103* gene and the kanamycin-resistance cassette into the *slr2031* region. The complete segregation of the *slr2031* region was checked by PCR using the primer pair of 2031-F and 2031-R (Table S3).

Culture conditions

The WT strains were grown photoautotrophically at 31°C in 50 mL of BG-11 medium containing 20-mM HEPES-NaOH, pH7.0, in test tubes (3 cm in diameter) with bubbling of air under continuous illumination at 20-μmol photons $m^{-2}s^{-1}$. The Δ*2103* strain was generated by insertion of a kanamycin-resistance cassette at the NsiI site of the coding region (10), and the ox-*2103* strain was grown under the same conditions, except that 20-μg mL^{-1} of kanamycin was added to the medium. Cell density was estimated by the optical density at 730 nm (OD_{730}) using a spectrophotometer (UV-1800; Shimadzu, Japan). For lipid analysis, each culture was adjusted at initial OD_{730}= 0.3 and cultivated under HL conditions of 200-μmol photons $m^{-2}s^{-1}$ for 3 or 7 days.

TLC

The extraction of total lipids from the defined amount of culture (10-mg CDW) was performed according to the method described by Bligh and Dyer (29). TLC analyses of neutral lipids were performed as described in Tanaka et al. (10).

MS analysis of the lipid fraction

The analyses of lipids containing in TAG-like spots with LC–MS/MS (LCMS-8030, Shimadzu) were performed as described in Tanaka et al. (10). For qualitative analysis (Q3 and product ion scanning), the samples were separated with a Shim-Pack XR-C8 column (2.2 μm, 75 mm × 2.0 mm i.d., Shimadzu) held at 40°C using solvent A, methanol/acetonitrile/5-mM ammonium formate, and solvent B, 2-propanol/acetonitrile/5-mM ammonium formate at a flow rate 0.2 mL min^{-1} with a binary gradient from 0 to 100% B in 20 min and 100% B kept for further 20 min. For quantitative analysis, analytes were separated using Shim-Pak XR-ODS II (2.2 μm, 75 mm × 2.0 mm i.d., Shimadzu) held at 40°C and a binary elution gradient consisting of tetrahydrofuran (THF)/methanol/5 mM ammonium formate (3:2:5, *v*/*v*/*v*) containing 0.1% formic acid as solvent C and THF/methanol/5 mM ammonium formate (7:2:1, *v*/*v*/*v*) containing 0.1% formic acid as solvent D. The flow rate was 0.2 mL min^{-1} with gradient condition as follows: 0 min, 70% D; 13 min, 100% D; 18 min, 100% D; 18.1 min, 70% D; and 20 min, 70% D. The transitions of $(M + NH_4)^+$ to (M–fatty acid + H)$^+$ for TAGs and $(M + NH_4)^+$ to (fatty acid+H_2O)$^+$ for acyl PQHs were used as precursor/product ion pairs in positive ionization mode. ESI was used for the ionization of TAG and acyl PQH, and APCI was used for free PQH_2 and PQ. Alkaline treatment of the TAG-like fraction was conducted in chloroform/methanol/1 N KOH (1:4:2, *v*/*v*/*v*) for 1 h at 42°C. Free PQH_2 and PQ were prepared from S.6803 WT cells and analyzed by LC–MS/MS according to Kayama et al. (13). Acetylation was conducted in acetic anhydride/pyridine (2:1) for 30 min at 50°C.

For GC–MS analysis, the extract from the TAG-like spot was treated firstly with 5% HCl in methanol for 1 h at 85°C. The methanolized lipids were extracted using hexane, dried under a N_2 flow, and treated secondly with BSTFA + 1% TMCS (Sigma) for 20 min at 100°C. Peaks of fatty acid methyl esters and TMS-phytol were determined by the MS spectra and comparison with authentic standards.

NMR analysis

The ^1H and ^{13}C NMR spectra in $CDCl_3$, using $(CH_3)_4Si$ ($\delta = 0$) as an internal reference, were recorded on a Bruker Avance 400 spectrometer with CryoProbe.

Visualization of neutral lipids in cyanobacterial cells

To 1 mL of cells cultivated under HL conditions for 3 or 7 days, 40 μL of 25% glutaraldehyde was added and incubated for 5 min. Cells were pelleted at 4,000 × g for 5 min, washed twice with TBS buffer, and suspended with 100 μL of TBS buffer. One μL of BODIPY 493/503 (Thermo Fisher Scientific, USA) stock solution (50 μg mL^{-1}) was added and incubated for 15 min. Cells were pelleted at 4,000 × g for 5 min, washed once with TBS buffer, and suspended with 300 μL of TBS buffer. Fluorescence microscopy was performed as described previously (10). The area of BODIPY fluorescence per cell was measured from digital images using the software Image J.

TEM

Electron microscopy was performed as described previously (28, 30). The same cyanobacterial cultures that were used for BODIPY staining were used for TEM observation.

Isolation of the NL fraction

NL fraction was isolated from cell extracts (50-mg CDW) using sucrose density gradient centrifugation according to the protocol for isolation of lipid droplets from bacterial cells such as *Rhodococcus* sp. RHA1 (31) and *N. punctiforme* (7) with slight modification as described in Tanaka et al. (10). Subsequent TLC and LC–MS/MS analyses were also performed as described previously (10).

Acknowledgments

We thank Prof. Karl Forchhammer (University of Tübingen) for the helpful discussion on storage compounds in cyanobacteria. The NMR and TEM analyses were performed using a Bruker Avance 400 spectrometer and a Hitachi H-7500 transmission electron microscope, respectively, installed at the Comprehensive Analysis Center for Science, Saitama University.

Supplementary material

Supplementary material is available at *PNAS Nexus* online.

Funding

This work was funded by the Nagase Science and Technology Foundation (to Y.H.).

Author contributions

T.I. and Y.H. designed the research; T.I., S.T., R.T., T.F., and K.A. performed the research; T.I., S.T., R.T., T.F., K.A., Y.K., and Y.H. analyzed the data; and T.I. and Y.H. wrote the paper.

Data availability

All data generated or analyzed during this study are included in this published article and its supplementary information files.

References

1 Kawahara A, Hihara Y. 2021. Biosynthesis of fatty acid derivatives by cyanobacteria: from basics to biofuel production. *Cyanobacteria Biotechnology* 12:331–368.
2 Röttiga A, Steinbüchel A. 2013. Acyltransferases in bacteria. *Microbiol Mol Biol Rev*. 77:277–321.
3 Ansari S, Fatma T. 2016. Cyanobacterial polyhydroxybutyrate (PHB): screening, optimization and characterization. *PLoS One* 11:e0158168.
4 Koch M, Doello S, Gutekunst K, Forchhammer K. 2019. PHB is produced from glycogen turn-over during nitrogen starvation in *Synechocystis* sp. PCC 6803. *Int J Mol Sci*. 20:1942.
5 Taranto PA, Keenan TW, Potts M. 1993. Rehydration induces rapid onset of lipid biosynthesis in desiccated *Nostoc commune* (Cyanobacteria). *Biochim Biophys Acta*. 1168:228–237.
6 Ramadan MF, Asker MMS, Ibrahim ZK. 2008. Functional bioactive compounds and biological activities of *Spirulina platensis* lipids. *Czech J Food Sci*. 26:211–222.
7 Peramuna A, Summers ML. 2014. Composition and occurrence of lipid droplets in the cyanobacterium *Nostoc punctiforme*. *Arch Microbiol*. 196:881–890.
8 Hauf W, Schmid K, Gerhardt ECM, Huergo LF, Forchhammer K. 2016. Interaction of the nitrogen regulatory protein GlnB (PII) with biotin carboxyl carrier protein (BCCP) controls acetyl-CoA levels in the cyanobacterium *Synechocystis* sp. PCC 6803. *Front Microbiol*. 7:1700.
9 Santana-Sánchez A, Lynch F, Sirin S, Allahverdiyeva Y. 2021. Nordic cyanobacterial and algal lipids: triacylglycerol accumulation, chemotaxonomy and bioindustrial potential. *Physiol Plant* 173:591–602.
10 Tanaka M, *et al*. 2020. Quantitative and qualitative analyses of triacylglycerol production in the wild-type cyanobacterium *Synechocystis* sp. PCC 6803 and the strain expressing AtfA from *Acinetobacter baylyi* ADP1. *Plant Cell Physiol*. 61:1537–1547.
11 Aizouq M, *et al*. 2020. Triacylglycerol and phytyl ester synthesis in *Synechocystis* sp. PCC 6803. *Proc Natl Acad Sci USA* 117:6216–6222.
12 Shih PM, *et al*. 2013. Improving the coverage of the cyanobacterial phylum using diversity-driven genome sequencing. *Proc Natl Acad Sci USA* 110:1053–1058.
13 Kayama M, *et al*. 2020. A non-photosynthetic green alga illuminates the reductive evolution of plastid electron transport systems. *BMC Biol*. 18:126.
14 Mène-Saffrané L, Jones AD, DellaPenna D. 2012. Plastochromanol-8 and tocopherols are essential lipid-soluble antioxidants during seed desiccation and quiescence in *Arabidopsis*. *Proc Natl Acad Sci USA* 107:17815–17820.
15 Perez R, Forchhammer K, Salerno G, Maldener I. 2016. Clear differences in metabolic and morphological adaptations of akinetes of two *Nostocales* living in different habitats. *Microbiology* 162:214–223.
16 Nierzwicki-Bauer SA, Balkwill DL, Stevens SE Jr. 1983. Three-dimensional ultrastructure of a unicellular cyanobacterium. *J Cell Biol*. 97:713–722.
17 van de Meene AML, Hohmann-Marriott MF, Vermaas WFJ, Roberson RW. 2006. The three-dimensional structure of the cyanobacterium *Synechocystis* sp. PCC 6803. *Arch Microbiol*. 184:259–270.
18 Liberton M, Austin JR, Berg RH, Pakrasi HB. 2011. Unique thylakoid membrane architecture of a unicellular N_2-fixing cyanobacterium revealed by electron tomography. *Plant Physiol*. 155:1656–1666.
19 Lundquist PK, Shivaiah K-K, Espinoza-Corral R. 2020. Lipid droplets throughout the evolutionary tree. *Prog Lipid Res*. 78:101029.
20 Mori-Moriyama N, Yoshitomi T, Sato N. 2023. Acyl plastoquinol is a major cyanobacterial substance that co-migrates with triacylglycerol in thin-layer chromatography. *Biochem Biophys Res Commun*. 641:18–26.
21 Liu Q, Siloto RMP, Lehner R, Stone SJ, Weselake RJ. 2012. Acyl-CoA:diacylglycerol acyltransferase: molecular biology, biochemistry and biotechnology. *Prog Lipid Res*. 51:350–377.
22 Rottet S, Besagni C, Kessler F. 2015. The role of plastoglobules in thylakoid lipid remodeling during plant development. *Biochim Biophys Acta*. 1847:889–899.
23 Gaude N, Bréhélin C, Tischendorf G, Kessler F, Dörmann P. 2007. Nitrogen deficiency in *Arabidopsis* affects galactolipid composition and gene expression and results in accumulation of fatty acid phytyl esters. *Plant J*. 49:729–739.
24 Panda B, Jain P, Sharma L, Mallick N. 2006. Optimization of cultural and nutritional conditions for accumulation of poly-β-hydroxybutyrate in *Synechocystis* sp. PCC 6803. *Bioresour Technol*. 97:1296–1301.
25 Kacmar J, Carlson R, Balogh SJ, Srienc F. 2006. Staining and quantification of poly-3-hydroxybutyrate in *Saccharomyces cerevisiae* and *Cupriavidus necator* cell populations using automated flow cytometry. *Cytometry A*. 69:27–35.
26 Koch M, *et al*. 2020. Maximizing PHB content in *Synechocystis* sp. PCC 6803: a new metabolic engineering strategy based on the regulator PirC. *Microb Cell Fact*. 19:231.
27 Řezanka T, Lukavský J, Siristova L, Sigler K. 2012. Regioisomer separation and identification of triacylglycerols containing vaccenic and oleic acids, and α- and γ-linolenic acids, in thermophilic cyanobacteria *Mastigocladus laminosus* and *Tolypothrix* sp. *Phytochemistry* 78:147–155.
28 Yamauchi Y, Kaniya Y, Kaneko Y, Hihara Y. 2011. Physiological roles of the cyAbrB transcriptional regulator pair Sll0822 and Sll0359 in *Synechocystis* sp. strain PCC 6803. *J Bacteriol*. 193:3702–3709.
29 Bligh EG, Dyer WJ. 1959. A rapid method of total lipid extraction and purification. *Can J Biochem Physiol*. 37:911–917.
30 Nitta K, Nagayama K, Danev R, Kaneko K. 2009. Visualization of BrdU-labelled DNA in cyanobacterial cells by Hilbert differential contrast transmission electron microscopy. *J Microscopy* 234:118–123.
31 Ding Y, *et al*. 2012. Identification of the major functional proteins of prokaryotic lipid droplets. *J Lipid Res*. 53:399–411.